

# Implicit vs Explicit Renormalization and Effective Interactions

E. Ruiz Arriola

*Departamento de Física Atómica, Molecular y Nuclear and Instituto Carlos I de Física Teórica y Computacional,  
Universidad de Granada, E-18071 Granada, Spain*

S. Szpigel

*Faculdade de Computação e Informática, Universidade Presbiteriana Mackenzie, Brazil*

V. S. Timóteo

*Grupo de Óptica e Modelagem Numérica (GOMNI), Faculdade de Tecnologia, Universidade Estadual de Campinas - UNICAMP, Brazil*

---

## Abstract

Effective interactions can be obtained from a renormalization group analysis in two complementary ways. One can either explicitly integrate out higher energy modes or impose given conditions at low energies for a cut-off theory. While the first method is numerically involved, the second one can be solved almost analytically. In both cases we compare the outcoming effective interactions for the two nucleon system as functions of the cut-off scale and find a strikingly wide energy region where both approaches overlap, corresponding to relevant scales in light nuclei  $\Lambda \lesssim 200\text{MeV}$ . This amounts to a great simplification in the determination of the effective interaction parameters.

---

## 1. Introduction

Since half a century ago the idea of effective interactions has been strongly pursued after the pioneering works by Goldstone [1], Moshinsky [2] and Skyrme [3]. They suggested to use this notion to cut down the complexity of the Nuclear Many Body Problem due to strong short range repulsion which arises when nucleon-nucleon (NN) interactions are probed at sufficiently high energies. Effective interactions were profitably exploited in the mid 70's [4] and have reached a high degree of sophistication (for a review see e.g. [5]). A very recent compilation of parameters is given in Ref. [6] displaying a huge diversity, somewhat reflecting the disparate phenomena which are used to fix the effective Hamiltonian, but remarkably exhibiting no link to the fundamental two-body interaction. In a recent work [7] (see also [8]) a model independent and implicit way of determining the effective interactions from NN low energy scattering data has been suggested. They depend on the minimal de Broglie wavelength between nucleons in a finite nucleus, a trend consistent with fitting coarse grained NN interactions [9] to fixed upper center of mass (CM) momenta [10].

In the last decade there has been an intense reformulation of the nuclear many body problem inspired by the Wilsonian renormalization group ideas providing an alternative approach to the determination of effective interactions [11, 12, 13] (for reviews see e.g. [14, 15, 16] and references therein) and their

characterization as finite cut-off counterterms [17]. This framework takes advantage of the proper momentum scale resolution or cut-off  $\Lambda$ , separating explicitly what degrees of freedom and interactions behave dynamically below that scale. The requirement that observables should be cut-off independent determines the implicit  $\Lambda$  dependence of the effective interaction. A direct and explicit way to achieve such interaction uses the Similarity Renormalization Group (SRG) method with a block-diagonal generator whence an effective hermitean phase-equivalent interaction is derived [18].

In the present paper we analyse the Block-Diagonal Similarity Renormalization Group (BD-SRG) scheme [18] as applied to the two body problem. This allows to implement by a continuous and unitary evolution in a momentum-dimension auxiliary parameter  $\lambda$ , referred to as the SRG-cutoff, a block-diagonal separation of the Hilbert space in two orthogonal (decoupled) subspaces  $\mathcal{H} = \mathcal{H}_P \oplus \mathcal{H}_Q$  which are below or above  $\Lambda$  respectively. The evolution runs from  $\lambda = \infty$  (the ultraviolet limit) to  $\lambda = 0$  (the infrared limit) and interpolates between a bare Hamiltonian,  $H_{\lambda=\infty}$ , and the block-diagonal one  $H_{\lambda=0}$  in a unitary way  $H_{\lambda=0} = UH_{\lambda=\infty}U^\dagger$ . This is the unitary implementation [18] to all energies of the previously proposed  $V_{\text{low } k}$ -approach [11] where the higher energy states are missing, and in practice a free theory was assumed above the energy determined by the momentum cut-off  $\Lambda$ , hence generating a truncation error. For the rest of the paper we will refer to this  $\Lambda$  as the  $V_{\text{low } k}$ -cutoff to be identified with the block-diagonal SRG one. We emphasize that a complete Hilbert space separation corresponds to the limit  $\lambda \rightarrow 0$ .

Although this block-diagonal scheme solves the problem as

---

*Email addresses:* earriola@ugr.es (E. Ruiz Arriola), szpigel@mackenzie.br (S. Szpigel), varese@ft.unicamp.br (V. S. Timóteo)

a matter of principle, SRG equations are differential equations in the SRG-cut-off  $\lambda$  for unbound operators defined on the Hilbert space, and they have only been solved exactly for simple cases [19]. For most cases however, SRG equations must be numerically posed on a finite  $N$ -dimensional momentum grid,  $p_n$ , and the differential equations require a further grid in the SRG-cut-off  $\lambda_i$  which introduces two infrared resolution scales  $\Delta p_n$  and  $\Delta \lambda_i$ . In the BD-SRG equations  $\Lambda$  takes values on the momentum grid  $p_n$ . The interplay among these scales makes the limit  $\lambda \leq \Delta p, \Lambda$  numerically stiff and computationally expensive. We will show that this infrared behaviour is best reproduced by directly using low energy scattering data in the continuum and, most remarkably, that effective interactions are accurately determined this way in a wide cut-off range.

## 2. Bare and effective interaction

We review briefly the renormalization problem for the two-nucleon system from a Wilsonian point of view to introduce our notation in a way that our results can be easily stated ( see e.g. Ref. [20] for an alternative set up). To motivate the discussion let us consider NN scattering, where one solves the Lippmann-Schwinger (LS) equation for the *bare* potential  $V$ . Taking the case of S-waves we have for the half-off-shell  $K$ -matrix,

$$K(p', p) = V(p', p) + \frac{2}{\pi} \int_0^\infty dq \frac{q^2 V(p', q)}{p^2 - q^2} K(q, p) \quad (1)$$

where  $K(p', p)$  is the reaction matrix which relation to the phase-shifts is given by

$$\frac{\tan \delta(p)}{p} = -K(p, p) \quad (2)$$

The effective interaction  $V_\Lambda(p', p)$  corresponds to a self-adjoint operator,  $V_\Lambda(p', p) = V_\Lambda(p, p')^*$ , acting in a reduced model Hilbert space with  $p, p' \leq \Lambda$  and fulfills

$$K_\Lambda(p', p) = V_\Lambda(p', p) + \frac{2}{\pi} \int_0^\Lambda dq \frac{q^2 V_\Lambda(p', q)}{p^2 - q^2} K_\Lambda(q, p). \quad (3)$$

Using the similar definition of Eq. (2) we get

$$\delta_\Lambda(p) = \delta(p) \Theta(\Lambda - p). \quad (4)$$

The idea is that by using this truncation one can work in a smaller space, without explicit reference to high energy states. This does not provide a unique definition of the effective interaction, so an auxiliary condition must be specified. In the original  $V_{\text{lowk}}$  approach [21] the half-off shell T-matrix was fixed to the bare one, a procedure which did not guarantee a self-adjoint operator, and hence a subsequent hermitization procedure was required. In the BD-SRG approach [18] the hermiticity is preserved along the SRG evolution.

The SRG method does not specify what the bare interaction should be and is usually taken as a realistic potential which fits NN data up to pion-production threshold,  $\Lambda \lesssim \sqrt{m_\pi M_N} \sim 400 \text{ MeV}$ . This introduces a long high momentum tail due to the short range repulsion which complicates the numerical convergence when solving the SRG flow equations. For illustration

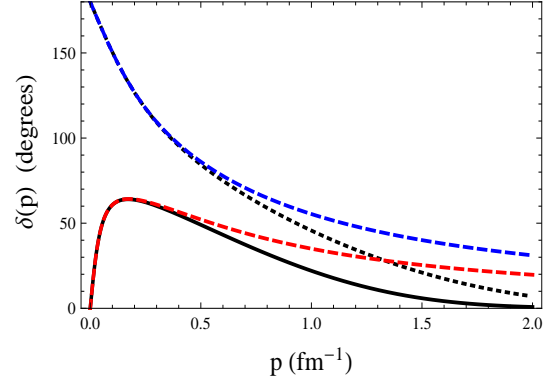


Figure 1:  $^1S_0$  (solid) and  $^3S_1$  (dotted) phase-shifts in degrees for the separable potential and compared with the effective range expansion to second order (dashed) as a function of the CM momentum (in  $\text{fm}^{-1}$ ).

purposes we take as the *bare* interaction the simple separable potential for the NN S-waves

$$V_\alpha(p, p') = C_\alpha g_\alpha(p') g_\alpha(p) \quad \alpha = ^1S_0, ^3S_1 \quad (5)$$

leading to the phase-shifts

$$\begin{aligned} p \cot \delta_\alpha(p) &= -\frac{1}{V_\alpha(p, p)} \left[ 1 - \frac{2}{\pi} \int_0^\infty dq \frac{q^2}{p^2 - q^2} V_\alpha(q, q) \right] \\ &= -\frac{1}{\alpha_0} + \frac{1}{2} r_0 p^2 + v_2 p^4 + \dots \end{aligned} \quad (6)$$

where in the last line a low momentum Effective Range Expansion (ERE) has been carried out and the scattering length  $\alpha_0$ , the effective range  $r_0$  and the  $v_2$  parameter have been introduced. Parameters in Eq. (5) are adjusted to reproduce  $\alpha_0$  and  $r_0$  which for a gaussian form factor  $g_\alpha(p) = e^{-p^2/L^2}$  are listed in Table 1. The resulting phase-shifts are presented in Fig. 1 together with the ERE results, which reproduce well data up to  $p \leq \Lambda_{\text{ERE}} \sim 100 \text{ MeV}$ . While they only resemble NN phase-shifts of the most recent Partial Wave Analysis [22] at low momenta, these two channels illustrate Levinson's theorem that  $\delta(0) - \delta(\infty) = n\pi$  with  $n$  the number of bound states and  $n_{^1S_0} = 0$  and  $n_{^3S_1} = 1$ . The pole of the  $^3S_1$  scattering amplitude at  $p = i\gamma = i0.2314 \text{ fm}^{-1}$  gives a satisfactory deuteron binding energy  $E_d = -\gamma^2/M = -2.22 \text{ MeV}$ .

Parameter	$\alpha_0$	$r_0$	$C$	$L$
Units	(fm)	(fm)	(fm)	( $\text{fm}^{-1}$ )
$^1S_0$	-23.74	2.77	-1.9158	0.6913
$^3S_1$	5.42	1.75	-2.3006	0.4151

Table 1: Model parameters for the gaussian separable potential  $V_\alpha(p', p) = C_\alpha e^{-(p^2 + p'^2)/L^2}$  used in the calculations.

## 3. Explicit Renormalization: Block diagonal evolution

The SRG method developed by Glazek and Wilson [23, 24] and independently by Wegner [25] (for a review see e.g. [26]) is based on a non-perturbative flow equation that governs the

unitary evolution of a hamiltonian  $H = T_{\text{rel}} + V$  with a flow parameter  $s$  that ranges from 0 to  $\infty$ ,

$$\frac{dH_s}{ds} = [\eta_s, H_s], \quad (7)$$

where  $\eta_s = [G_s, H_s]$  is an anti-hermitian operator that generates the unitary transformations. We take the Block-diagonal SRG generator [18] given by

$$G_s = H_s^{\text{BD}} \equiv \begin{pmatrix} PH_sP & 0 \\ 0 & QH_sQ \end{pmatrix}. \quad (8)$$

where  $P$  and  $Q = 1 - P$  are projection operators. The flow parameter  $s$  has dimensions of  $[\text{energy}]^{-2}$  and in terms of a similarity cutoff  $\lambda$  with dimension of momentum is given by the relation  $s = \lambda^{-4}$ . The flow equation is to be solved with the boundary condition  $H_s|_{s \rightarrow s_0} \equiv H_{s_0}$ . Using that  $T_{\text{rel}}$  is independent of  $s$ , we obtain

$$\frac{dV_s}{ds} = [\eta_s, H_s]. \quad (9)$$

In a partial-wave relative momentum space basis, the projection operators are determined in terms of a momentum cutoff scale  $\Lambda$  that divides the momentum space into a low-momentum  $P$ -space ( $p < \Lambda$ ) and a high-momentum  $Q$ -space ( $p > \Lambda$ ),

$$P \equiv \theta(\Lambda - p); \quad Q \equiv \theta(p - \Lambda). \quad (10)$$

The potential  $V_s$  can be written as,

$$V_s \equiv \begin{pmatrix} PV_sP & PV_sQ \\ QV_sP & QV_sQ \end{pmatrix}. \quad (11)$$

By choosing the block-diagonal generator, the matrix-elements inside the off-diagonal blocks  $PV_sQ$  and  $QV_sP$  are suppressed as the flow parameter  $s$  increases (or as the similarity cutoff  $\lambda$  decreases), such that the hamiltonian is driven to a block-diagonal form,

$$\lim_{\lambda \rightarrow 0} V_\lambda = PV_{\text{lowk}}P + QV_{\text{highk}}Q = \begin{pmatrix} V_{\text{lowk}} & 0 \\ 0 & V_{\text{highk}} \end{pmatrix} \quad (12)$$

Thus, in the limit  $\lambda \rightarrow 0$  the  $P$ -space and the  $Q$ -space become completely decoupled. Thus, while unitarity implies  $\delta_\lambda(p) = \delta(p)$  for any  $\lambda$  one has

$$\lim_{\lambda \rightarrow 0} \delta_\lambda(p) = \delta_{\text{lowk}}(p) + \delta_{\text{highk}}(p) \quad (13)$$

where  $\delta_{\text{lowk}}(p) = \delta(p)\theta(\Lambda - p)$  and  $\delta_{\text{highk}}(p) = \delta(p)\theta(p - \Lambda)$  are the phase shifts of the  $V_{\text{lowk}}$  and  $V_{\text{highk}}$  potentials respectively (see Eq. (4)).

#### 4. Implicit Renormalization: Low cut-off evolution

At low cut-offs  $\Lambda$  we may approximate the hermitian effective interaction by a polynomial,

$$\begin{aligned} V_\Lambda(p', p) &= C_0 + C_2(p^2 + p'^2) \\ &+ C_4(p^4 + p'^4) + C_4'p^2p'^2 + \dots \end{aligned} \quad (14)$$

where  $C_0, C_2, C_4, C_4', \dots$  are *real* coefficients depending on  $\Lambda$  to be determined. This corresponds to an Effective Field Theory (EFT) with contact interactions only. We expect Eq. (14) to hold up to  $p, p' \leq \Lambda_{\text{ERE}}$ . Using the potential of Eq. (14) the LS Eq. (3) reduces to a system of algebraic equations which solution is well known (see e.g. Ref. [21]). At lowest leading order (LO) we just keep the leading term  $C_0$  and get

$$C_0(\Lambda) = \frac{\alpha_0}{1 - \frac{2\Lambda\alpha_0}{\pi}}, \quad (15)$$

showing that  $\lim_{\Lambda \rightarrow 0} V_\Lambda(0, 0) = \alpha_0$ . Going to Next-to-leading order (NLO) we obtain

$$\begin{aligned} -\frac{1}{\alpha_0\Lambda} &= \frac{4(-2c_2^2 + 90\pi^4 + 15(3c_0 + 2c_2)\pi^2)}{9\pi(c_2^2 - 10c_0\pi^2)}, \\ r_0\Lambda &= \frac{16(c_2^2 + 12\pi^2c_2 + 9\pi^4)}{\pi(c_2 + 6\pi^2)^2} - \frac{12c_2(c_2 + 12\pi^2)}{(c_2 + 6\pi^2)^2} \frac{1}{\alpha_0\Lambda} \\ &+ \frac{3c_2\pi(c_2 + 12\pi^2)}{(c_2 + 6\pi^2)^2} \frac{1}{\alpha_0^2\Lambda^2}, \end{aligned} \quad (16)$$

where  $c_0 = 4\pi\Lambda C_0$ ,  $c_2 = 4\pi\Lambda^3 C_2$ . In the second equation we have eliminated  $C_0$  in terms of  $\alpha_0$ . This leads for any cut-off  $\Lambda$  to the mapping  $(\alpha_0, r_0) \rightarrow (C_0, C_2)$ . At this level of approximation there are two branches and we choose the one consistent with the LO one for  $\Lambda \rightarrow 0$ , see Eq. (15) and Fig. 2. We will denote LO by  $C_0^{(0)}$  and NLO by  $C_0^{(2)}$  and  $C_2^{(2)}$ . One should note that in the case of the  $^3S_1$  channel  $C_0^{(0)}$  is singular and the derivatives of  $C_2^{(0)}$  and  $C_2^{(2)}$  are discontinuous at  $\Lambda = \pi/2\alpha_0 \sim 0.3 \text{ fm}^{-1}$ , which is the momentum scale where the deuteron bound-state appears. The strong resemblance of both  $^1S_0$  and  $^3S_1$  at the scales around  $\Lambda \sim 1 \text{ fm}^{-1}$  is just a reminiscent of the SU(4) Wigner symmetry for the two-nucleon system [7, 27, 28, 29].

One can in principle improve by including more terms beyond second order in Eq. (14). The problem is that there are two such terms  $C_4$  and  $C_4'$  [21] but there is only *one* low energy parameter in the ERE,  $v_2$  in Eq. (6). This is so because scattering does not depend just on the on-shell potential. Thus, the implicit renormalization is not unique beyond NLO. This is just a manifestation of the ambiguities of the inverse scattering problem which can only be fixed after three or higher body properties are taken into account<sup>1</sup>. Clearly, and even for the  $C_0$  and  $C_2$  coefficients, increasing  $\Lambda$  values one starts seeing more high energy details of the theory.

Even at NLO the question is how small must be the cut-off scale so that Eq. (14) works. There is a maximum value  $\Lambda_{\text{WB}}$  for the cutoff scale  $\Lambda$  above which one cannot fix the strengths of the contact interactions  $C_2^{(0)}$  and  $C_2^{(2)}$  by fitting the experimental values of both the scattering length  $\alpha_0$  and the effective range  $r_0$  while keeping the renormalized potential hermitian. This limit corresponds to the Wigner causality bound realized as an off-shell unitarity condition [21, 31]. Indeed, for

<sup>1</sup>Actually from a dimensional point of view the two-body operators with four derivatives are suppressed as compared to contact three body operators. The off-shellness of the two body problem can be equivalently be translated into some three-body properties [30].

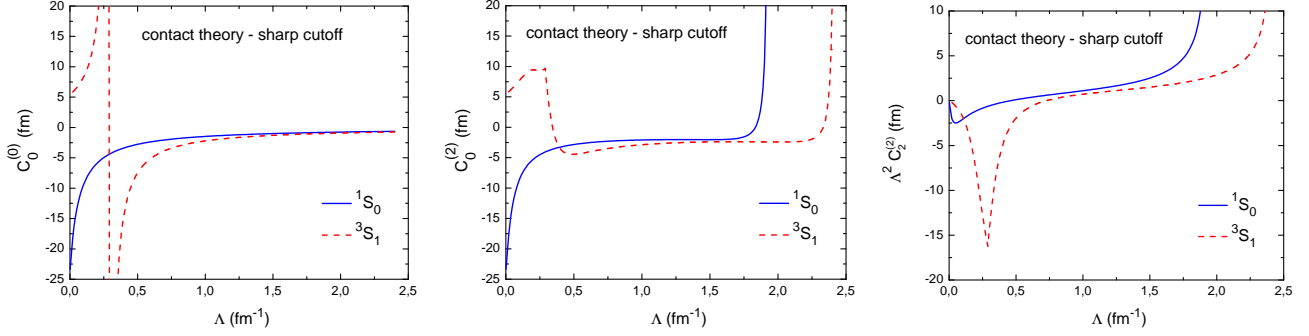


Figure 2:  $C_0^{(0)}$ ,  $C_2^{(0)}$  and  $C_2^{(2)}$  for the contact theory in the continuum regulated by a sharp momentum cutoff for the  $^1S_0$  channel and the  $^3S_1$  channel. The parameters are determined from the solution of the  $LS$  equation for the on-shell  $K$ -matrix by fitting the ERE parameters

$\Lambda > \Lambda_{\text{WB}} \sim 1.9 \text{ fm}^{-1}$  in the case of the  $^1S_0$  channel and  $\Lambda > \Lambda_{\text{WB}} \sim 2.4 \text{ fm}^{-1}$  in the case of the  $^3S_1$  channel, the parameters  $C_2^{(0)}$  and  $C_2^{(2)}$  diverge before taking complex values and hence violating the hermiticity of the effective potential in Eq. (14).

## 5. Numerical results

The Block-Diagonal-SRG equations, Eq.(9), have to be solved numerically on a momentum grid with  $N$ -points yielding  $4 \times N^2$  non-linear first order coupled differential equations. Furthermore, an auxiliary numerical cut-off  $P_{\text{max}} = N\Delta p$  must also be introduced. It is interesting to test the space dimensions needed to solve the contact theory close to the continuum. This is shown in Fig. 3 where one sees that large  $N$  is needed to reproduce the continuum limit. We will set  $N = 50$  and  $P_{\text{max}} = 5 \text{ fm}^{-1}$  to our SRG calculations, solve the system of  $4 \times N^2$  non-linear first-order coupled differential equations by using an adaptive fifth-order Runge-Kutta algorithm as in Ref. [31] and compare the results to the contact interaction with the same  $N$  and  $P_{\text{max}}$ . We check unitarity by comparing phase-shifts along the  $\lambda$  evolution,  $\delta_\lambda(p) = \delta(p)$ . The sharp momentum projectors in Eq. (10) may be regularized as smooth projectors [32] ( $Q \equiv 1 - P$ )

$$P = \Theta(\Lambda - p) = \lim_{n \rightarrow \infty} e^{-(p/\Lambda)^n}, \quad (17)$$

and we will take the values  $n = 2, 4, 8, 16$  to check convergence. We want to compare the running of the coefficients  $C_0$  and  $C_2$  with the cut-off  $\Lambda$  in the contact theory potential at NLO to the running of the corresponding coefficients  $\tilde{C}_0$  and  $\tilde{C}_2$  with the  $V_{\text{low k}}$  cutoff ( $\equiv \Lambda$ ) extracted from a polynomial fit of the BD-SRG-evolved gaussian potential,

$$V_{\Lambda, \Lambda}(p, p') = \tilde{C}_0 + \tilde{C}_2 (p^2 + p'^2) + \dots \quad (18)$$

The parameters  $C$  and  $L$  in the initial gaussian potential ( $\lambda, \Lambda \rightarrow \infty$ ), defined by Eq. (5), and the coefficients  $C_0$  and  $C_2$  in the contact theory potential at NLO are determined from the solution of the  $LS$  equation for the  $K$ -matrix on the finite momentum grid by fitting the experimental values of the scattering length  $a_0$  and the effective range  $r_0$ . The coefficients  $\tilde{C}_0$

and  $\tilde{C}_2$  are determined by fitting the diagonal matrix-elements of the BD-SRG-evolved potential for the lowest momenta with the polynomial form and the finite momentum grid <sup>2</sup>.

In Fig. 4 we show the results for  $\tilde{C}_0$  and  $\Lambda^2 \tilde{C}_2$  extracted from the  $^1S_0$  channel and the  $^3S_1$  channel BD-SRG-evolved gaussian potentials on a grid (with  $N = 50$  gauss points and  $P_{\text{max}} = 5 \text{ fm}^{-1}$ ) and down to the lowest SRG cutoff  $\lambda = 0.1 \text{ fm}^{-1}$ , compared to  $C_0$  and  $\Lambda^2 C_2$  obtained for the contact theory potential at NLO (on the same grid) regulated by a smooth exponential momentum cutoff with sharpness parameter  $n = 16$ . As we see, there is a remarkably good agreement between the coefficients extracted from the BD-SRG-evolved potential and those obtained for the contact theory in the limit  $\lambda \rightarrow 0$ .

It is important to point out that the agreement between the running of the coefficients  $C_0$  and  $C_2$  in the contact theory potential and the running of the coefficients  $\tilde{C}_0$  and  $\tilde{C}_2$  extracted from the BD-SRG-evolved gaussian potential as the similarity cutoff  $\lambda$  decreases below  $\Lambda$  can be traced to the decoupling between the  $P$ -space and the  $Q$ -space, which follows a similar pattern. Thus, in the limit  $\lambda \rightarrow 0$  we expect to achieve a high degree of agreement for cutoffs  $\Lambda$  up to  $\Lambda_{\text{WB}}$  determined by the Wigner bound for the contact theory.

The overlap between the discretized explicit and implicit numerical solutions is verified in a wide range of cut-offs  $\Lambda$ . If continuum accuracy was to be judged from the slow convergence pattern of Fig. 3, the equivalent BD-SRG calculations would be out of question. Thus, the continuum limit  $\Delta p \rightarrow 0$  is better and more simply represented by the implicit approach.

For the  $^1S_0$  and  $^3S_1$  neutron-proton scattering states this range is within  $0.5 \text{ fm}^{-1} \leq \Lambda \leq 1.5 \text{ fm}^{-1}$ . This is a welcome feature, since it suggests that the bulk of the effective interaction and its scale dependence can directly be extracted from low energy NN data, as done in Ref. [7], where the Skyrme force parameters deducible solely from the NN interaction in S- and P-waves were determined.

It is interesting to determine the role played by OPE in the implicit method in the cut-off range around  $\Lambda \sim m_\pi$  but below pion production threshold  $\Lambda \lesssim \sqrt{m_\pi M_N}$  as OPE is an

<sup>2</sup>Actually, looking for a fiducial region to extract  $C_0$  and  $C_2$  in the explicit method when  $\Lambda \geq \Lambda_{\text{ERE}}$  requires allowing for higher order polynomial contributions.

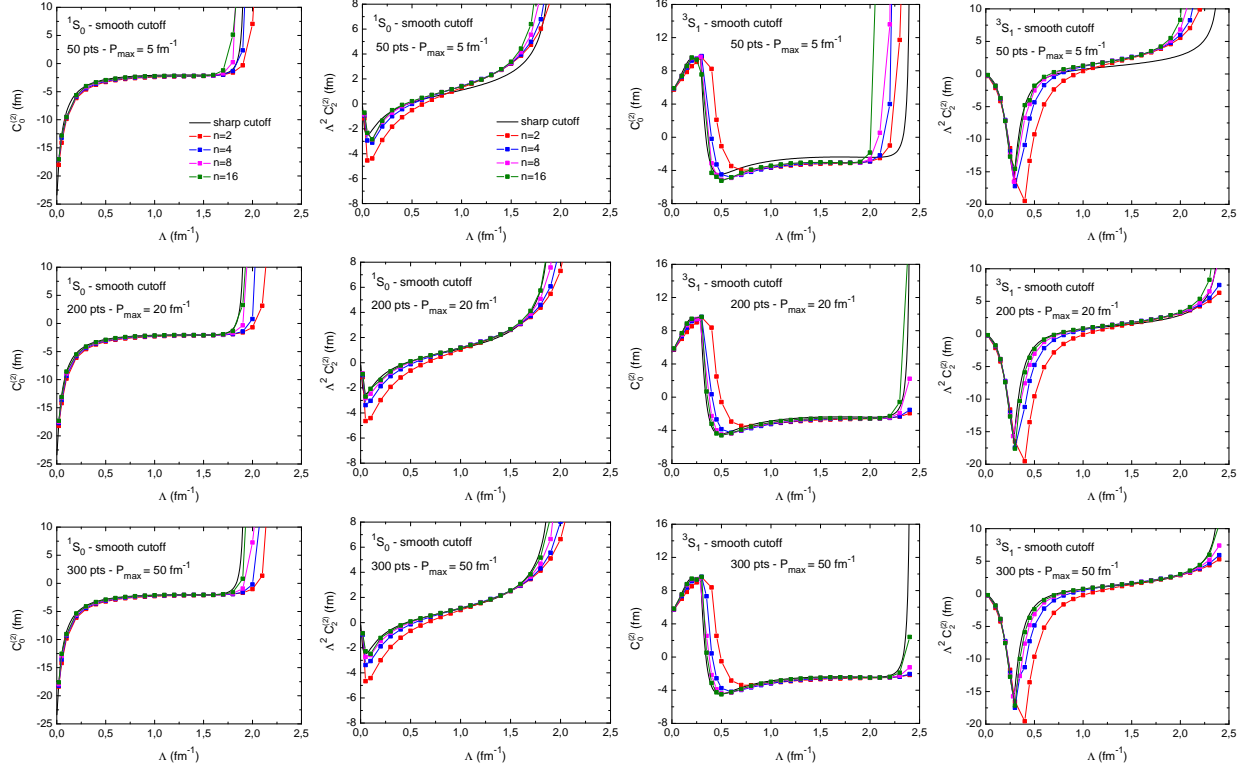


Figure 3:  $C_0^{(2)}$  and  $C_2^{(2)}$  for the contact theory on a grid regulated by a smooth exponential momentum cutoff for the  $^1S_0$  channel and the  $^3S_1$  channel  $NN$  potentials at NLO. For comparison, we also show the corresponding  $C_0^{(2)}$  and  $C_2^{(2)}$  for the contact theory in the continuum regulated by a sharp momentum cutoff. In both cases the parameters are determined from the solution of the  $LS$  equation for the on-shell  $K$ -matrix by fitting the ERE parameters.

indispensable ingredient of realistic bare interactions (see e.g. Ref. [33]). According to the recent Partial Wave Analysis of Ref. [22] of about 8000 pp and np data, OPE is the only needed contribution for  $r > 3$  fm. If one separates the initial condition as  $V_{\lambda=\infty} = V_{r \leq 3\text{fm}} + V_{1\pi, r \geq 3\text{fm}} \equiv V_S + V_L$  one has  $V_L \equiv V_{1\pi, r \geq 3\text{fm}} \ll V_S \equiv V_{r \leq 3\text{fm}}$  and one can attempt a perturbative expansion of the block-SRG evolved potential. Thus, evolving the full  $V$  and just  $V_S$  we find from Eq. (9) that  $PV_{\text{low-k}}P = PV_{S,\text{low-k}}P + PV_LP + \mathcal{O}(V_L^2)$ . Using the  $\delta$ -shell representation of Ref. [22] we get that the accuracy of this perturbation theory in the  $^1S_0$  channel is indeed small;  $\mathcal{O}(V_L^2) \leq 10^{-2}\text{fm}$  for  $2.1 \geq \Lambda \geq 0.5\text{fm}^{-1}$  at  $p, p' \leq \Lambda$ . This suggests that the unevolved (and  $\Lambda$ -independent) long distance OPE piece ( $r \geq 3\text{fm}$ ) remains small after evolution and this contribution can be treated perturbatively. A more complete analysis of this important issue will be presented elsewhere.

The block diagonal SRG reduces the model space but also induces a truncation error for decreasing  $\Lambda$ . The SRG evolves the bare hamiltonian to a lower similarity cutoff  $\lambda$ . Due to the unitarity, the SRG evolution to a lower similarity cutoff  $\lambda$  preserves the EFT truncation errors for a given  $V_{\text{low-k}}$  cutoff  $\Lambda$ .

We have shown with a simple example the situation with S-waves. Higher partial waves, such as P-waves are in better shape. The scale saturation displayed by the implicit method in Ref. [7] becomes more pronounced in this case (see Eq.(12) in that paper). It remains to be seen what is the actual situation

when the implicit method is applied to interactions describing  $NN$  scattering data to higher energies. Work along these lines is in progress.

## 6. Conclusions

While the effective interaction idea is very appealing there is no unique way to define it; its definition depends on *how* are the high and low energies separated and *what* is the relevant energy scale cut-off. Within a given scheme, however, the cut-off scale dependence of effective interactions representing a given bare interaction in a model space can be carried out in two complementary ways: either explicitly from a Block-Diagonal SRG transformation or implicitly by using scattering data and renormalization conditions. Although the complementarity of both explicit and implicit views of the renormalization procedure is often invoked on general grounds, we note that it is seldomly tested within the present context of nuclear effective interactions. As we have shown such a test requires to pin down the numerics in a finite momentum grid with sufficient accuracy making the explicit BD-SRG method computationally expensive and impractical. At low energies effective interactions and their scale dependence are just given by counterterms evaluated for finite cut-offs. We find a remarkably wide range of cut-offs where this complementarity holds in a model independent way. This suggests that the implicit renormalization approach

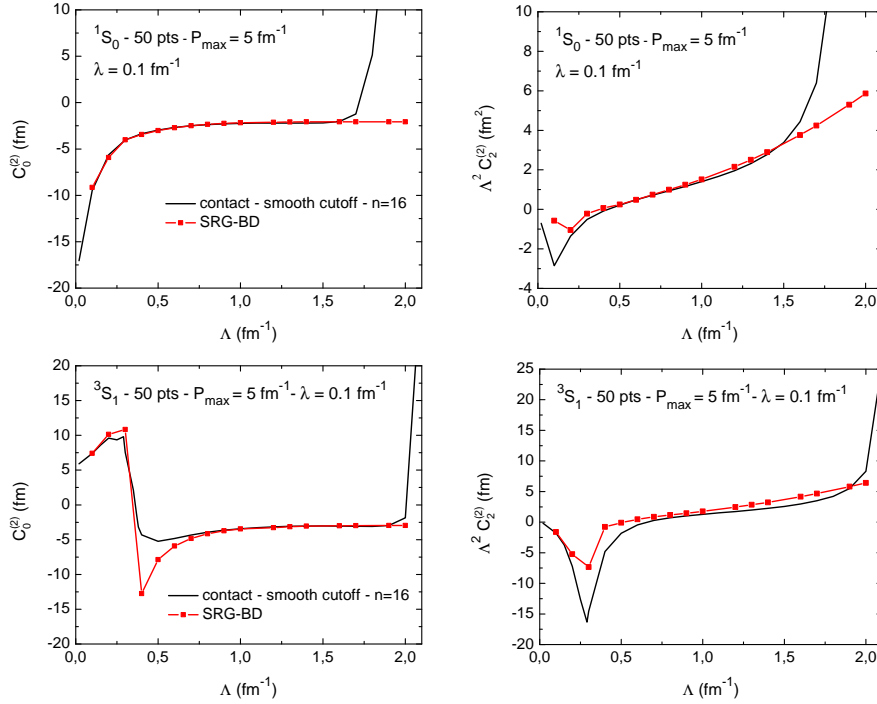


Figure 4:  $C_0$  and  $C_2$  as a function of the block-diagonal cutoff  $\Lambda$  extracted from the  $^1S_0$  and  $^3S_1$  channels gaussian potential on a grid (with  $N = 50$  gauss points and  $P_{\max} = 5 \text{ fm}^{-1}$ ) evolved through the SRG transformation with the block-diagonal generator for the lowest SRG cutoff  $\lambda = 0.1 \text{ fm}^{-1}$ . For comparison, we also show  $C_0$  and  $C_2$  for the  $^1S_0$  and  $^3S_1$  channels contact theory potential at NLO (on the same grid) regulated by a smooth exponential momentum cutoff with  $n = 16$ .

may be a simpler, more accurate and direct method to determine the effective interaction than the explicit and traditional method based on numerically integrating the operator SRG flow equations using as initial condition a phenomenological bare interaction fitted to NN scattering data below pion production threshold. Another related issue is the role played by three-, four-body etc. properties in the definition of two body effective interactions as this becomes necessary for a truly model independent formulation of effective interactions.

E.R.A. was supported by Spanish DGI (grant FIS2011-24149) and Junta de Andalucia (grant FQM225). S.S. was supported by Instituto Presbiteriano Mackenzie and FAPESP. V.S.T. would like to thank FAEPEX, FAPESP and CNPq for financial support. Computational power provided by FAPESP grant 2011/18211-2.

## References

- [1] J. Goldstone, Proc.Roy.Soc.Lond.A Math.Phys.Eng.Sci. **239**, 267 (1957).
- [2] M. Moshinsky, Nuclear Physics **8**, 19 (1958), ISSN 0029-5582.
- [3] T. Skyrme, Nucl. Phys. **9**, 615 (1959).
- [4] D. Vautherin and D. M. Brink, Phys. Rev. **C5**, 626 (1972).
- [5] M. Bender, P.-H. Heenen, and P.-G. Reinhard, Rev. Mod. Phys. **75**, 121 (2003).
- [6] M. Dutra, O. Lourenco, J. Sa Martins, A. Delfino, J. Stone, et al., Phys.Rev. **C85**, 035201 (2012), 1202.3902.
- [7] E. Ruiz Arriola (2010), nucl-th/1009.4161.
- [8] S. X. Nakamura Prog.Theor.Phys. **114**, 77 (2005),
- [9] R. Navarro Perez, J. Amaro, and E. Ruiz Arriola, Prog.Part.Nucl.Phys. **67**, 359 (2012), 1111.4328.
- [10] R. Navarro Perez, J. Amaro, and E. Ruiz Arriola, Few Body Syst. **54**, 1487 (2013).
- [11] S. K. Bogner, T. T. S. Kuo, A. Schwenk, D. R. Entem, and R. Machleidt, Phys. Lett. **B576**, 265 (2003),
- [12] S. K. Bogner, T. T. S. Kuo, and A. Schwenk, Phys. Rept. **386**, 1 (2003).
- [13] S. Bogner, R. Furnstahl, and R. Perry, Phys.Rev. **C75**, 061001 (2007).
- [14] L. Coraggio, A. Covello, A. Gargano, N. Itaco, and T. T. S. Kuo, Prog. Part. Nucl. Phys. **62**, 135 (2009), 0809.2144.
- [15] S. K. Bogner, R. J. Furnstahl, and A. Schwenk, Prog. Part. Nucl. Phys. **65**, 94 (2010), 0912.3688.
- [16] R. Furnstahl and K. Hebeler (2013), 1305.3800.
- [17] J. D. Holt, T. T. S. Kuo, G. E. Brown, and S. K. Bogner, Nucl. Phys. **A733**, 153 (2004), nucl-th/0308036.
- [18] E. Anderson et al., Phys. Rev. **C77**, 037001 (2008), 0801.1098.
- [19] S. Szpigel and R. J. Perry (1999), nucl-th/9906031.
- [20] K. Harada, K. Inoue, and H. Kubo, Phys.Lett. **B636**, 305 (2006).
- [21] D. Entem, E. Ruiz Arriola, M. Pavon Valderrama, and R. Machleidt, Phys.Rev. **C77**, 044006 (2008).
- [22] R. Navarro Perez, J. Amaro, and E. Ruiz Arriola Phys.Rev. **C88**, 024002 (2013).
- [23] S. D. Glazek and K. G. Wilson, Phys. Rev. **D48**, 5863 (1993).
- [24] S. D. Glazek and K. G. Wilson, Phys. Rev. **D49**, 4214 (1994).
- [25] F. J. Wegner, Physics Reports **348**, 77 (2001).
- [26] S. Kehrein, *The flow equation approach to many-particle systems* (Springer, 2006).
- [27] A. Calle Cordon and E. Ruiz Arriola, Phys. Rev. **C78**, 054002 (2008).
- [28] V.S. Timóteo, S. Szpigel, and E. Ruiz Arriola, Phys.Rev. **C86**, 034002 (2012), 1108.1162.
- [29] E. Ruiz Arriola, V. S. Timóteo, and S. Szpigel, PoS CD **12**, 106 (2013), nucl-th/1302.3978.
- [30] A. Amghar and B. Desplanques, Nucl.Phys. **A585**, 657 (1995).
- [31] S. Szpigel, V. S. Timóteo, and F. d. O. Duraes, Annals Phys. **326**, 364 (2011), 1003.4663.
- [32] S. Bogner, R. Furnstahl, S. Ramanan, and A. Schwenk, Nucl.Phys. **A784**, 79 (2007), nucl-th/0609003.
- [33] K. Harada, H. Kubo, and Y. Yamamoto, Phys.Rev. **C83**, 034002 (2011).